Title: Mechanical, thermal and swelling properties of Cellulose Nanocrystals/PVA nanocomposites membranes

Authors: Zaib Jahan, Muhammad Bilal Khan Niazi, Øyvind Weiby Gregersen

PII: S1226-086X(17)30432-X
DOI: http://dx.doi.org/doi:10.1016/j.jiec.2017.08.014
Reference: JIEC 3562

To appear in:

Received date: 30-6-2017
Revised date: 2-8-2017
Accepted date: 6-8-2017

Please cite this article as: Zaib Jahan, Muhammad Bilal Khan Niazi, Øyvind Weiby Gregersen, Mechanical, thermal and swelling properties of Cellulose Nanocrystals/PVA nanocomposites membranes, Journal of Industrial and Engineering Chemistryhttp://dx.doi.org/10.1016/j.jiec.2017.08.014

Mechanical, thermal and swelling properties of Cellulose Nanocrystals/PVA nanocomposites membranes

Zaib Jahan[a,b], Muhammad Bilal Khan Niazi[a,b], Øyvind Weiby Gregersen[b,*]

[a]School of Chemical and Materials Engineering, National University of Sciences and Technology, Islamabad, Pakistan

[b]Department of Chemical Engineering, Norwegian University of Science and Technology, Norway

*Corresponding Author: oyvind.w.gregersen@ntnu.no (Øyvind Weiby Gregersen)

Tel.: +47-73594029

Postal address: Department of Chemical Engineering, Norwegian University of Science and Technology, Norway

Graphical abstract

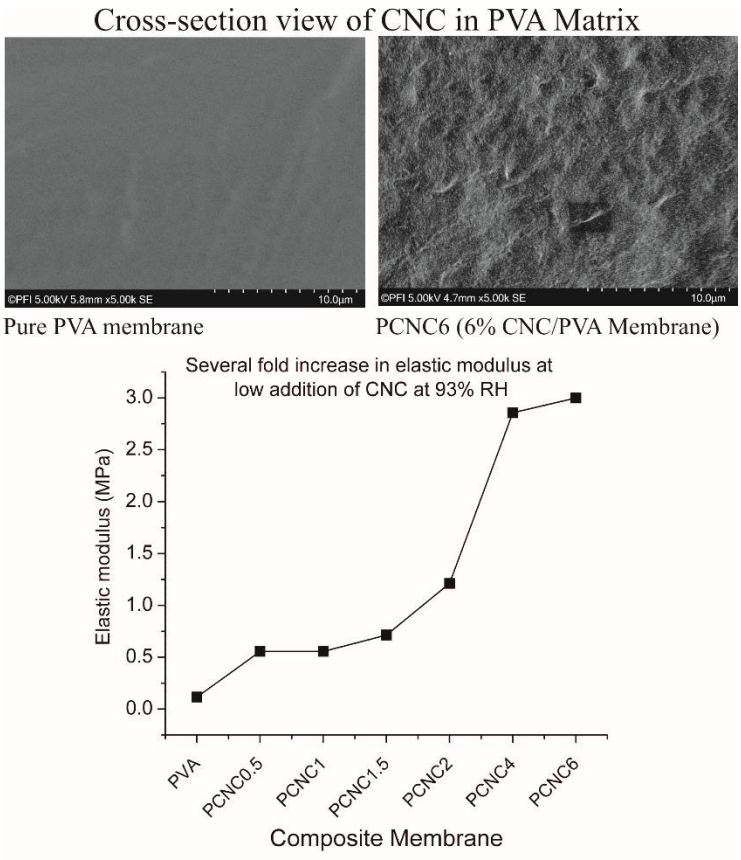

Abstract

Cellulose nanocrystals (CNC) have strong reinforcing properties when incorporated in a compatible polymer matrix. The study was conducted to investigate the effect of addition of different proportions of CNC on the mechanical, thermal and swelling properties of poly(Vinyl alcohol) (PVA) nanocomposite membranes for biogas separation. The incorporation of CNC in PVA increased the crystallinity at all investigated relative humidities. No apparent trend is observed for mechanical properties for dry membranes (0% RH) with addition of CNC in PVA matrix. However, at 93% RH the elastic modulus increased 25 times with addition of CNC compared to pure PVA membranes. Moreover, tensile strength also showed twice the values at

53% RH and 93% RH after the addition of CNC. Membranes containing higher CNC content absorbed 9% less moisture. Swelling, thermal and mechanical properties indicate a good potential of CNC/PVA nanocomposite membranes for use in CO_2 separation membranes.

Keywords: Crystalline nanocellulose; Poly(vinyl alcohol); Mechanical strength; Dynamic Mechanical properties; Thermogravimetric analysis.

1. Introduction

The natural fiber-reinforced polymer composites are considered as a possible environmental friendly alternative to petroleum-based, non-biodegradable polymeric materials [1, 2]. Much research has been done to replace synthetic fillers used in composite materials. Synthetic fillers cause environmental concerns due to the end-of-life disposal, their partial combustibility and he high demand on techniques for recycling of the materials [3]. One of the possible solutions is to replace the synthetic fillers with natural ones, such as cellulose fibers, starch or chitin. They offer biodegradability, low cost, low density, and good thermal and mechanical properties to composite materials [4].

Cellulose is the most abundantly available biodegradable and renewable natural polymer in the ecosystem. Cellulose fiber consists of nano-sized microfibrils, which are further divided into amorphous (CNF) and crystalline parts (crystalline nano-cellulose) [5, 6]. The cellulose material has high stiffness and structural strength due to the presence of hydrogen bonding between its

chains [2]. Some of the well-known characteristics of nanocellulose are low density, high length-to-diameter ratio, high mechanical strength and high specific surface area [7]. Moreover, abundant hydroxyl groups are present on the surface of nano-cellulose making it possible to perform surface modifications like esterification, silylation or polymer grafting, to functionalize nanocellulose and facilitate its dispersion into different polymer matrices [8]. Due to all these properties, nanocellulose has attracted a great deal of interest in scientific and industrial research compared to traditional cellulosic fibers and oil based materials.

Cellulose nanocrystals (CNC) are stiff, rod-like particles having a width of about 2-30 nm and can be several hundreds of nanometers in length [9]. They are usually prepared by strong acid hydrolysis of a cellulose source such as hardwood pulp [10], microcrystalline cellulose [11], cotton [12], wheat straw [13, 14], algae [15] or sugar beet [16]. The amorphous part of nanocellulose is dissolved [8]. Furthermore, ultrasonic-assisted (2,2,6,6-tetramethylpiperidin-1-yl)oxyl (TEMPO) oxidation, ammonium persulfate oxidation, and sequential oxidation and reductive amination can also be used to produce CNCs [7]. Much effort has been committed to the use of CNC's as reinforcing agent in polymeric matrices [17]. CNC consists of highly crystalline rod-like particles with high specific area [18]. The strong interaction between adjacent CNC's by hydrogen bonding was proposed to explain its excellent barrier, electrical and mechanical properties. Furthermore, it has great potential to be used as reinforcing agent in various synthetic and natural polymers [7, 19]. CNC has shown good characteristics when compared with Kevlar, carbon fibers, stainless steel, or bulk materials [20, 21].

PVA is the prime water soluble synthetic polymer produced in the world. It is prepared by hydrolysis of polyvinyl acetate and is widely used and studied as a nanocomposite material [22]. PVA is more environment friendly and feasible alternative to polymers as polyethylene [23].

Moreover, PVA has good thermal stability, optical properties and oxygen barrier properties. PVA composites are widely used in different applications including filters [24], packaging [25], tissue engineering scaffolds [26] and CO_2 membrane separation [27]. Nanocellulose has been incorporated with PVA as a reinforcing agent in different applications demanding high mechanical strength and stiffness along with great degree of swelling i.e. polymeric membranes [27], films [28], and fibers [29].

PVA nanocellulose composite membranes are a serious candidate for CO_2 separation. Strong inter-fibrillar bonds present in nanocellulose can form a dense network, and be used as barrier material [27, 30]. Nano-cellulose fibers may also form porous ultra- absorbent materials like aerogels and foams, because of its high strength and low weight. Crystalline cellulose cannot absorb water but water can penetrate into amorphous parts of its structure causing swelling and water will adsorb to the surface of the nano-cellulose particles [31]. Between CNF and CNC, films of CNC show high degree of swelling, due to presence of charged sulfate groups on the surface [32].

One of the most important criteria for the selection of hydrogel membranes is its swelling behavior. Swelling changes the physical and chemical structure of the polymers. The affinity between solvent and polymer increase the polymer swelling, which leads to an increase in the free volume. The membrane structure becomes more open and permits dissolved molecules to pass through in gas separation, influencing both permeability and selectivity [27]. Similarly, swelling also has an impact on the mechanical properties of the hydrogel membranes.

Keeping this background, the overall objective of this work is to develop and characterize novel crystalline nanocellulose (CNC)/PVA nanocomposite membranes for potential application in CO_2 separation. The thermal and morphological properties of CNC/PVA composite membranes

were investigated using TGA, DSC and SEM, respectively. The crystallinity index and molecular interactions between CNC/PVA matrixes were calculated by XRD and FTIR. The mechanical properties were determined at high degree of swelling using DMA and mechanical testing. In this context, the applicability of such films in CO_2 membrane separation field has been adjudged with respect to their moisture uptake and mechanical properties.

2. Experiments

2.1 Materials

Polyvinyl alcohol (M_W 89000-124000 and 87-89 % hydrolyzed) and crystalline nanocellulose (CNC) was purchased from Sigma Aldrich. The average length and the width of CNC was 130 nm ± 67 nm and 5.9 nm ± 1.8 nm, respectively. Thus the aspect ratio was 23 ± 12 [33]. Distilled water was used throughout the experimentation.

2.2 Methods

2.2.1. Preparation of PVA nanocomposite membranes reinforced with CNC

The granules of PVA (see Table 1) were dissolved in distilled water and stirred at 90 °C for 3 hrs. Afterwards, the solution was left rolling at room temperature overnight. Different proportions of CNC (Table 1) suspension with known solid content were added to the prepared PVA solution. The resulting suspension was stirred at 800 rpm overnight at room temperature. The final suspension was sonicated for 10 minutes at 60 Watt. The obtained suspensions were cast in

polypropylene petri dishes and dried for 1 week at ambient room temperature. The resulting membranes were conditioned in a desiccator at 0 % RH before further characterization.

3. Characterization

3.1 Fourier transform infrared (FTIR) spectroscopy

A Thermo Nicolet Nexus FTIR spectrometer equipped with an attenuated total reflectance (ATR) device was used to record the FTIR spectra of all synthesized composite membranes in the region of 800-4000 cm^{-1}. All the resulting FTIR spectra were compared on the bases of intensity and shift of vibrational bands to evaluate the effects of CNC amount on PVA composite membranes.

3.2 Moisture uptake

The moisture uptake was gravimetrically analyzed for a step change from 0% RH to two different relative humidities i.e. 53% RH and 93%RH, for all the composite membranes. Measurements were taken every day until the equilibrium was established. [34, 35].

3.3 X-ray diffraction (XRD)

Bruker D8 Focus X-Ray Diffractometer equipped with a LynxEye™ super-speed detector was used to study the crystalline structures of the composite membranes. The system was operated at 40 kV and 40mA using Cu radiation exhibiting a wavelength of 1.5418Å. The samples were scanned between 10° 2θ to 50° 2θ. The step size and scan speed were kept at

0.02°2θ and 2 s/step, respectively. The crystallinity index of the membrane was calculated as reported in literature using [36]. The integration of peaks was done by using software program Origin 8.1. The area under the curve from 10° to 50° in the XRD spectrum was considered as total area.

3.4 Scanning electron microscopy (SEM)

Surface and cross-sectional morphology of the nanocomposite membranes with varying proportion of CNC were investigated using a Hitachi SEM SU 3500 (Japan) with an acceleration voltage of 5 kV. For surface morphology, the samples were sputter-coated with a thin layer of gold to prevent the build of an electrostatic charge. While for cross sectional analysis, the samples were freeze-cracked using liquid nitrogen to investigate the distribution of nanocellulose within PVA matrix. The composite membranes were soaked in liquid nitrogen for 10 seconds. Then, each sample was fractured immediately to get a freeze-fractured surface. Before the SEM observation was done on the sample membrane, the cross-section surface of the fractured film was sputter-coated with a gold layer [2].

3.5 Thermal Analysis

3.5.1 Thermogravimetric analysis (TGA)

TGA was carried out using a thermogravimetric analyser (TGA, Q500, Thermal). 8–10 mg of the nanocomposite membranes were placed in open aluminum pans and heated 10 °C/min from room temperature to 700 °C. The weight change in relation to temperature and decomposition temperature (T_{dec}) was studied [34].

3.5.2 Differential scanning calorimetry (DSC)

Differential scanning calorimetery (DSC, TA Q100, Thermal Scientific) was used to investigate the glass transition temperature (*Tg*), cold crystallization and melting temperature of the samples. 10 mg for each sample was put in an aluminum pan covered with a proper lid. An empty pan was also used together as standard in the DSC sample holder and was scanned at a rate of 10 °C/min from 30 to 250 °C, under N_2 atmosphere. The scanning process involved an initial heating followed by cooling, and finally a second temperature scanning was executed [37].

3.6 Mechanical Properties

3.6.1 Mechanical testing

The mechanical properties [tensile strength (TS), % elongation at break (% Eb) and tensile modulus] of nanocomposite membranes were determined using Zwick Roell tensile testing equipment. Five specimens of each composition were tested at, 25 ^{o}C, in accordance with ASTM D638. The dimensions of the test specimens were as follows: length 50 mm, width 15 mm and thickness 0.1 ± 0.02 mm. The crosshead speed used was 50 mm/min. Three different relative humidity levels, i.e. 0% RH, 53% RH and 93% RH at 25 °C were used to condition the sample for four days. The thickness and width of the samples were measured before testing. The results were presented as the average of five measurements.

3.6.2 Dynamic Mechanical analysis (DMA)

Dynamic Mechanic Analyzer 242(NETZSCH-Gerätebau GmbH) with liquid N_2 cooling system was used to investigate the dynamic mechanical properties of nanocomposite membranes with varying CNC proportion. The temperature range was -20 ^oC to 120 ^oC at a heating rate of 2 ^oC/min. The measurements were done at a constant frequency of 1Hz. The sample dimensions are 20 mm (length), 5 mm (width) and 0.1-0.2 mm (thickness). All prepared samples were conditioned for four days at two relative humidities i.e. 0% RH, and 93% RH, prior to testing.

4. Results and Discussion

4.1 Fourier transform infrared (FTIR) spectroscopy

The FTIR spectra of PVA/CNC nanocomposite membranes with varying concentration of CNC are depicted in Fig. 1. A band around 3280 cm^{-1} is observed in all spectra is assigned to the free O-H stretching vibration of the –OH groups. O-H stretching vibration from the intramolecular hydrogen bonds within the PVA and intermolecular hydrogen bonding between hydroxyl groups of PVA and the CNC are responsible for this band. The addition of CNC causes a shift towards higher wavenumber. The peak for C-H stretching vibrations from alkyl groups is present at 2919 cm^{-1} in all formulations. The peak around 1732 cm^{-1} is attributed to the C=O and –C-O stretching from the residual acetate groups in the PVA matrix [38]. However, the intensity of that peak was reduced with the addition of CNC.

The band at 1243 cm^{-1} is attributed to the C-O stretching vibration. Its intensity is inversely proportional to proportion of CNC. The reduction in peak intensity is due to the formation of hydrogen bonds between PVA and CNC [39, 40]. The peak at 1424.4 cm^{-1} is present in all the

spectra and ascribed to C-H deformation vibration. The bending vibration of the C-H bonds has caused vibration peaks at 1423 cm^{-1} and 1373 cm^{-1} in almost all spectra. Moreover, the addition of CNC resulted in red shift of the peak at 1373 cm^{-1}.

A double peak is observed in the region of 1086-1030 cm^{-1}. The peak at 1086 cm^{-1} corresponds to C-O stretching vibration [39, 40]. Moreover, the peak at 1033 cm^{-1} could be attributed to the C-H bending vibration of CH_2 group [41]. The second peak at 1033 cm^{-1} becomes sharper with the addition of CNC and reduces the intensity of first peak at 1086 cm^{-1}. This elaborates the potential interaction of PVA with nanocellulose [39, 40]. The absorption band at 834 cm^{-1} of PVA is gradually reduced with the increase of CNC. This phenomenon also supports the possible interaction between CNC and PVA [42].

4.2 Moisture uptake

Two different relative humidities i.e. 53% RH and 93% RH, were used to investigate the moisture uptake of all the nanocomposite membranes. Fig. 2 showed the % increase in the weight over 10 days due to absorption of moisture. At 53% RH, PVA/CNC membranes showed an increase in moisture absorption with small addition levels of CNC but reduced swelling at higher addition levels. All the composite membranes showed an increase in moisture uptake for the first four days. Afterwards, the weight stabilized and equilibrium was achieved. Addition of a small amount of CNC until 1.5% caused an increasing absorbance of moisture, however at higher CNC levels than 1.5% the moisture absorption was reduced. PCNC4 and PCNC6 absorbed even less moisture than the pure PVA membrane. The % weight increase compared to pure PVA is attributed to the hydrophilic nature of cellulose [7]. However, decrease in swelling

at higher proportion of CNC i.e. PCNC2, PCNC4 and PCNC6, is attributed to the reinforcing effect of the CNC. It acted as a cross-binder in a polymer, restraining the swelling mechanically Hence, resulting in a decrease of moisture uptake at higher nanocellulose addition levels.

At 93% RH, the rate of moisture uptake has been increased for all the composite membranes compared to 53% RH. PCNC0.5 absorbed maximum moisture i.e. 33.7%. Whereas, PCNC-6 showed minimum moisture uptake 24%. All synthesized membranes containing CNC showed less moisture uptake as compared to pure PVA membrane except PCNC0.5. The moisture uptake is caused by the same mechanism as described above. However, at higher humidity (93% RH), the reinforcement effect dominates at lower CNC level because the membrane swells more. Thus the resistance against swelling set up by the CNC becomes more important. The swelling at higher CNC content may also be reduced by the higher crystallinity of membranes with addition of CNC (see XRD results). It is important for CO_2 membrane separation to have maximum swelling at relatively high humidities i.e. 93% RH. So, lower CNC content in PVA/nanocellulose composite membranes seems most promising for high permeability for CO_2 separation.

4.3 X-ray diffraction (XRD)

Fig. 3 shows the XRD patterns of all the formulated nanocomposite membranes at three different relative humidities i.e. 0% RH, 53% RH and 93% RH. The crystallinity of Pure PVA crystals and PVA membranes was also calculated to evaluate the difference due to the membrane casting process. Peaks at 2θ value of 23° and 41°of PVA crystals are not present in PVA membrane. However, the characteristic peak of PVA at 19.5° is observed in all the formulations representing the (11O) plane of the semicrystalline region of partially hydrolyzed PVA [43]. At 0% RH, PVA

membrane has lower crystallinity as compared to pure PVA crystals. The incorporation of CNC into PVA nanocomposite membranes slightly reduced the intensity of the (11O) plane. However, the intensity of the peak at 2θ value of 23º has been increased at higher proportion of CNC. Even in PCNC4 and PCNC6, the intensity of the peak due to addition of CNC in PVA suppressed the PVA peak i.e.2θ value of 19º. The crystallinity of PVA nanocomposite membranes were directly proportional to CNC contents in formulations i.e. PCNC6 showed maximum crystallinity of 70 % and PCNC0.5 has lowest of 56.5 %. The peak of CNC at 2θ value of 22.5º (2OO plane) started appearing already at addition of 0.5% CNC (wt. /wt. PVA) and resulted in an increase of crystallinity even at lower CNC content.

Similar trends were observed at 53% RH and 93% RH. The percentage increase of crystallinity was directly proportional to CNC concentration in the PVA nanocomposite blends. The maximum crystallinity was obtained for PCNC6 at 53% RH and 93% RH i.e. 72% and 74% RH, respectively. This increase in crystallinity at higher concentrations of CNC and humidities was attributed to the contribution of both PVA and nanocellulose to the overall crystallinity. Furthermore, the addition of nanocellulose will also enhance the number of nucleating agents resulting in a higher quantity of small crystallites are bundled together [37].

4.4 Scanning electron microscopy (SEM)

The surface and cross-section of nanocomposite membranes were studied by SEM. Fig.4 (a,b & c) shows the surface and cross-section micrographs of pure PVA, PCNC1 and PCNC6 composite membranes. The surface of pure PVA membrane was plane. However, the surfaces became

rougher with addition of CNC (Fig. 4 b,c). Appreciable amount of aggregates was seen on the surface of membranes after addition of CNC. These aggregates have a wide size distribution. Moreover, the rate and size of aggregates are proportional to CNC content in the nanocomposite membranes. SEM micrograph of PCNC1 showed even distribution of CNC on PVA membrane surface. However, increase in concentration of CNC in PVA the matrix cause cluster formation (see Fig. 4c).

The cross-sectional surface of pure PVA and CNC reinforced PVA composite membranes were also examined. As described in literature, this examination was important to determine the distribution and interaction of nanocellulose within PVA matrix [2].

Even distribution of CNC in PVA matrix was observed in the cross-sectional micrographs at low concentration of CNC. However, with increase in CNC concentration cluster formation takes place. The mechanical properties of nanocomposite membranes highly depend on the distribution of the CNC in the PVA matrix [2]. The thickness of the nanocomposite membranes ranges between 137 μm to 157μm.

4.5 Thermal Analysis

4.5.1 Thermogravimetric analysis (TGA)

TGA and DTGA were used to examine the thermal stability of PVA and PVA/CNC nanocomposite membranes as shown in Fig. 5. Incorporation of CNC in the PVA matrix slightly reduced the thermal stability and introduced a fourth degradation peak in nanocomposite membranes. The results are in line with literature [2, 44]. The thermal stability of nanocomposite membranes changed directly proportionally to the CNC

proportion. The first stage (70 to 110 °C) of degradation could be associated to the evaporation of water. The rate of water evaporation increased with the addition of CNC. During the next two stages of thermal degradation i.e. between 200 to 260 °C and 300 to 350 °C, the nanocomposite membranes experienced a higher weight loss and rate than pure PVA membrane. The second degradation stage started at 223 °C for pure PVA membrane. The starting temperature of this stage was slightly reduced with addition of CNC. The lowest starting degradation temperature at this stage was observed for PCNC6 i.e. 196 °C. All the formulations with CNC got a new peak at a degradation temperature between 215 to 280 °C. This weight loss can be due to the structural degradation of CNC [37]. About 50 wt. % was lost in this region. The third degradation stage was observed in the range of 300 to 500 °C. Here again, a similar trend has been observed. The degradation temperature was slightly reduced after the addition of CNC proportion. Pure PVA observed degradation peak at 325 °C. Whereas, PCNC0.5 and PCNC1 showed degradation peaks at 323 and 320 °C, respectively. Minimum degradation temperature was observed for PCNC4 and PCNC6 i.e. 306 and 303 °C, respectively. The weight loss is above 90 wt. % (inclusive the previous losses) after this stage. The final degradation (above 400 °C) is ascribed to the decomposition of carbonaceous materials [34, 45]. Hence, addition of CNC in PVA matrix does only slightly reduce the thermal stability of the membranes in the relevant temperature range.

4.5.2 Differential scanning calorimetry (DSC)

The glass transition (Tg) temperatures, crystallization temperatures (Tc) and melting temperatures (Tm) of the PVA and PVA/CNC composite membranes were studied using

DSC. The DSC curves of all formulated composite membranes are presented in Fig. 6. The analysis was performed by a heating-cooling-heating cycle (H-C-H). The thermal history and moisture of the PVA composite systems are removed during the first heating cycle [37]. No consistent trend is observed for Tg after addition of CNC in PVA membranes. Firstly, Tg decreased with addition of small amount of CNC i.e. Tg for PVA is at 68.9 °C, whereas PCNC0.5 has at 61.8 °C. PCNC1 and PCNC1.5 also showed low value of Tg as compared to PVA i.e. 66 °C and 66.9 °C, respectively. However, PCNC2 observed higher Tg (72.1 °C) as compared to PVA. The first decrease in Tg with addition of small amounts of CNC is ascribed to the limitation of mobility of PVA chain segments by the adsorptive forces of the CNC [37]. Only PCNC6 and PCNC2 showed higher Tg values as compared to pure PVA membrane.

Similarly, the melting temperature did not show any trend with addition of CNC. The melting temperature remains between 234 ± 2 °C. However, the crystallization temperature (Tc) has increased with the addition of CNC. Tc of pure PVA membrane is at 118.8 °C, whereas the PCNC6 has at 189.5 °C. This increase in Tc with addition of CNC has been attributed to the difference of size and shape of crystals present in both cases. The more uniform (shape and size) crystals are present in the PVA membrane. The homogeneous phase nucleation dominates the formation of crystals during cooling in the pure PVA membrane. However, the phenomenon of crystallization is dictated by heterogeneous phase nucleation due to presence of CNC having large surface area [37].

4.6 Mechanical Properties

4.6.1 Tensile testing

Fig. 7 (a,b,c) presents the tensile properties of the PVA and PVA/CNC nanocomposite membranes at three different relative humidities i.e. 0%RH, 53%RH and 93%RH. At 0%RH and 53%RH the elastic modulus initially decreased with addition of CNC. However, at PCNC1.5 the elastic modulus started increasing at both relative humidities. At 53%RH and particularly at 93%RH the elastic modulus increases considerably with increasing nanocellulose concentration. The elastic modulus is much lower at 53%RH and particularly at 93%RH compared to 0% RH. This is attributed to higher water uptake at 53% RH and 93% RH after four days. The elastic modulus values at 93% RH are approx. 80% lower compared to 0% RH.

A similar trend was observed for tensile strength (TS) at 0%RH. Initially, with addition of CNC the TS started decreasing but after PCNC1.5, it increased. However, the TS is proportional to CNC concentration at 53% RH and 93% RH. The maximum value of TS is achieved for PCNC6 at 0%RH and 53% RH i.e. 155 MPA and 132 MPA, respectively. This increase in TS can be ascribed to high aspect ratio and high elastic modulus of cellulose increasing the E-modulus and tensile strength of the composite material. The effect is particularly strong at high moisture content when the E-modulus of PVA becomes very low. Increased crystallinity at greater proportion of CNC could also contribute to increased E-modulus and tensile strength.

Fig. 7(c) presents the effect of CNC concentration on the % elongation at break of PVA/CNC nanocomposite membranes. At 0%RH, all PVA/CNC membranes have an % elongation at break below 10 %. The % elongation at break slightly increased with addition of CNC in the PVA matrix. However, PCNC6 again showed low value at 0%RH. Furthermore, CNC content has no effect on the elongation of nanocomposite membranes at 53% RH and 93%

RH except PCNC6 at 53%RH. PCNC6 observed the lowest value of % elongation at break compared to all other formulations at 53% RH. However, all other formulations have similar value at their relative humidities.

The increase in relative humidity (93% RH as compared to 53%RH and 0%RH) led to a strong increase in elongation at break. The increase of elongation at break in higher relative humidities ascribed to higher moisture uptake. This results in broken intermolecular hydrogen bonds and increased polymer mobility. At 93% RH, membranes absorb almost 10 times more water compared to 53% RH after four days, which results in increase in elongation at break and decrease in strength. The decrease of elongation at breaks due to increase in CNC content can be attributed to the intramolecular or intermolecular hydrogen bonds of PVA with the nanocellulose [2].

4.6.2 Dynamic Mechanical analysis

The DMA analysis is conducted to explain the reinforcing effect brought by the addition of CNC in PVA matrix at different humidities. The temperature dependent storage modulus E' and tan δ for all formulated nanocomposite membranes are presented in Fig 8. The DMA analysis showed unexpected and scattered results particularly below Tg.

The storage modulus did not show a systematic trend with addition of CNC in the PVA matrix. PCNC2 showed highest storage modulus, whereas PVA and PCNC6 resulted in lowest. The Tg is strongly reduced with increasing humidity from approx. 37 ^{o}C at 0%RH to -9 C at 93%RH. At 93% RH, storage modulus for samples with PCNC has been increased compared to the pure PVA membrane. Moreover, huge drop in storage modulus is observed with increase in moisture content and temperature.

The tan δ has observed trends at both the humidities i.e. 0% RH and 93% RH. The height of tan δ peak decreased with addition of CNC at both investigated humidities. It can be ascribed to the restrictions imposed by nanofibrils against molecular motion of surface adsorbed polymer chains, resulting in more elastic response in the material [46, 47]. The tan δ value decreased with addition of CNC contents. The pure PVA membrane had the tan δ peak at 54 °C at 0% RH. This value is lower than Tg measured by DSC. The peak shifts to lower temperature on addition of nanocellulose at 0%RH, but the trend is less clear for 93% RH. At higher CNC proportion i.e. PCNC4 and PCNC6, proper peaks of tan δ has not been observed. That can be attributed to the high agglomeration rate of CNC in PVA matrix.

As the membranes are usually operated at high temperature and high moisture contents, the high storage modulus of the nanocomposite membranes with more CNC is very valuable.

5. Conclusions

The study was conducted to investigate the mechanical, thermal and swelling properties of PVA/CNC nanocomposite membranes with aid of tensile testing, DMA, TGA, DSC and moisture uptake to evaluate their potential for use in biogas separation. The addition of CNC in composite membranes dramatically increased the E-modulus at higher humidities. The crystallinity of nanocomposite membranes increased with addition of CNC. The maximum crystallinity is achieved at 6 wt.% concentration of CNC in PVA matrix at tested relative humidities. The moisture uptake increases for small additions of CNC, but is reduced at higher CNC proportion at 53% RH and 93% RH. SEM micrographs showed homogeneous distribution of CNC within PVA matrix at lower CNC concentration. However, cluster formation takes place

at higher CNC proportion. The thermal decomposition temperature of PVA/CNC composite membranes was slightly reduced at higher CNC contents. There are no important changes in glass transition temperature with addition of CNC. At 0% RH, addition of CNC showed no unique trend for mechanical properties. However, at higher humidities elastic modulus and mechanical strength are proportional to CNC content but % elongation at break remain constant. Low CNC content in PVA matrix resulted in good swelling, low crystallinity and improved E-modulus. Hence, addition of some 0.5 – 2 % (wt./wt. of PVA) CNC in PVA nanocomposite membranes can be a promising solution to obtain a good membrane for gas separations.

Funding

This research did not receive any specific funding agencies in the public, commercial, or not-for-profit sectors.

Acknowledgments

The authors would like to thank Magnus Rotan in Department of Material Science and Engineering of Norwegian University of Science and Technology for XRD analysis.

Reference

[1] W. Li, Q. Wu, X. Zhao, Z.H. Huang, J. Cao, J. Li, S.X. Liu, Carbohyd Polym, 113 (2014) 403-410.

[2] Y.C. Ching, A. Rahman, K.Y. Ching, N.L. Sukiman, C.H. Chuah, Bioresources, 10 (2015) 3364-3377.
[3] A. Bhatnagar, M. Sain, J Reinf Plast Comp, 24 (2005) 1259-1268.
[4] S.J. Eichhorn, C.A. Baillie, N. Zafeiropoulos, L.Y. Mwaikambo, M.P. Ansell, A. Dufresne, K.M. Entwistle, P.J. Herrera-Franco, G.C. Escamilla, L. Groom, M. Hughes, C. Hill, T.G. Rials, P.M. Wild, J Mater Sci, 36 (2001) 2107-2131.
[5] M.J. Cho, B.D. Park, J Ind Eng Chem, 17 (2011) 36-40.
[6] Y.C. Ching, T.S. Ng, Bioresources, 9 (2014) 6373-6385.
[7] J.A. Sirvio, S. Honkaniemi, M. Visanko, H. Liimatainen, Acs Appl Mater Inter, 7 (2015) 19691-19699.
[8] Y. Habibi, L.A. Lucia, O.J. Rojas, Chem Rev, 110 (2010) 3479-3500.
[9] H. Hakansson, P. Ahlgren, Cellulose, 12 (2005) 177-183.
[10] S. Beck-Candanedo, M. Roman, D.G. Gray, Biomacromolecules, 6 (2005) 1048-1054.
[11] D. Bondeson, A. Mathew, K. Oksman, Cellulose, 13 (2006) 171-180.
[12] W.J. Orts, J. Shey, S.H. Imam, G.M. Glenn, M.E. Guttman, J.F. Revol, J Polym Environ, 13 (2005) 301-306.
[13] W. Helbert, J.Y. Cavaille, A. Dufresne, Polym Composite, 17 (1996) 604-611.
[14] A. Dufresne, J.Y. Cavaille, W. Helbert, Polym Composite, 18 (1997) 198-210.
[15] T. Imai, C. Boisset, M. Samejima, K. Igarashi, J. Sugiyama, Febs Lett, 432 (1998) 113-116.
[16] A. Dufresne, J.Y. Cavaille, M.R. Vignon, J Appl Polym Sci, 64 (1997) 1185-1194.
[17] M.A.S.A. Samir, F. Alloin, J.Y. Sanchez, A. Dufresne, Polymer, 45 (2004) 4149-4157.
[18] P. Terech, L. Chazeau, J.Y. Cavaille, Macromolecules, 32 (1999) 1872-1875.
[19] M. Roohani, Y. Habibi, N.M. Belgacem, G. Ebrahim, A.N. Karimi, A. Dufresne, Eur Polym J, 44 (2008) 2489-2498.
[20] R.J. Moon, C.R. Frihart, T. Wegner, Forest Prod J, 56 (2006) 4-10.
[21] R.J. Moon, A. Martini, J. Nairn, J. Simonsen, J. Youngblood, Chem Soc Rev, 40 (2011) 3941-3994.
[22] B. Ramaraj, J Appl Polym Sci, 103 (2007) 909-916.
[23] M. Flieger, M. Kantorova, A. Prell, T. Rezanka, J. Votruba, Folia Microbiol, 48 (2003) 27-44.
[24] Y. Shang, Y.L. Peng, Desalination, 204 (2007) 322-327.
[25] P. Alexy, D. Kachova, M. Krsiak, D. Bakos, B. Simkova, Polym Degrad Stabil, 78 (2002) 413-421.
[26] K.H. Schmedlen, K.S. Masters, J.L. West, Biomaterials, 23 (2002) 4325-4332.
[27] L.Y. Deng, M.B. Hagg, J Membrane Sci, 363 (2010) 295-301.
[28] E.H. Qua, P.R. Hornsby, H.S.S. Sharma, G. Lyons, R.D. McCall, J Appl Polym Sci, 113 (2009) 2238-2247.
[29] A.J. Uddin, J. Araki, Y. Gotoh, Biomacromolecules, 12 (2011) 617-624.
[30] L.Y. Deng, T.J. Kim, M.B. Hagg, J Membrane Sci, 340 (2009) 154-163.
[31] A. Dufresne, Mater Today, 16 (2013) 220-227.
[32] K. Syverud, P. Stenius, Cellulose, 16 (2009) 75-85.
[33] S.N. Molnes, I.P. Torrijos, S. Strand, K.G. Paso, K. Syverud, Ind Crop Prod, 93 (2016) 152-160.
[34] M.B.K. Niazi, A.A. Broekhuis, Eur Polym J, 64 (2015) 229-243.
[35] S.D. Zhang, Y.R. Zhang, X.L. Wang, Y.Z. Wang, Starch-Starke, 61 (2009) 646-655.
[36] M.B.K. Niazi, M. Zijlstra, A.A. Broekhuis, Carbohyd Polym, 97 (2013) 571-580.
[37] A. Mandal, D. Chakrabarty, J Ind Eng Chem, 20 (2014) 462-473.
[38] P.S. Thomas, J.P. Guerbois, G.F. Russell, B.J. Briscoe, J Therm Anal Calorim, 64 (2001) 501-508.
[39] K. Choo, Y.C. Ching, C.H. Chuah, S. Julai, N.S. Liou, Materials, 9 (2016).
[40] H.M.P.N. Kumar, M.N. Prabhakar, C.V. Prasad, K.M. Rao, T.V.A.K. Reddy, K.C. Rao, M.C.S. Subha, Carbohyd Polym, 82 (2010) 251-255.
[41] A.A. Hamidu, B.A. Aliyu, T.J. B., S.A. Osemeahon, International Research Journal of Pure & Applied Chemistry, 6 (2015) 7.
[42] M.S. Peresin, Y. Habibi, J.O. Zoppe, J.J. Pawlak, O.J. Rojas, Biomacromolecules, 11 (2010) 674-681.

[43] J. Sriupayo, P. Supaphol, J. Blackwell, R. Rujiravanit, Carbohyd Polym, 62 (2005) 130-136.
[44] T.S. Ng, Y.C. Ching, N. Awanis, N. Ishenny, M.R. Rahman, Mater Res Innov, 18 (2014) 400-404.
[45] X. Jia, Y.F. Li, Q. Cheng, S.J. Zhang, B. Zhang, Eur Polym J, 43 (2007) 1123-1131.
[46] O. Chaabouni, S. Boufi, Carbohyd Polym, 156 (2017) 64-70.
[47] H. Dong, Y.R. Sliozberg, J.F. Snyder, J. Steele, T.L. Chantawansri, J.A. Orlicki, S.D. Walck, R.S. Reiner, A.W. Rudie, Acs Appl Mater Inter, 7 (2015) 25464-25472.

Caption of Figures:

Fig. 1. FT-IR spectra of PVA and PVA/CNC composite membranes.

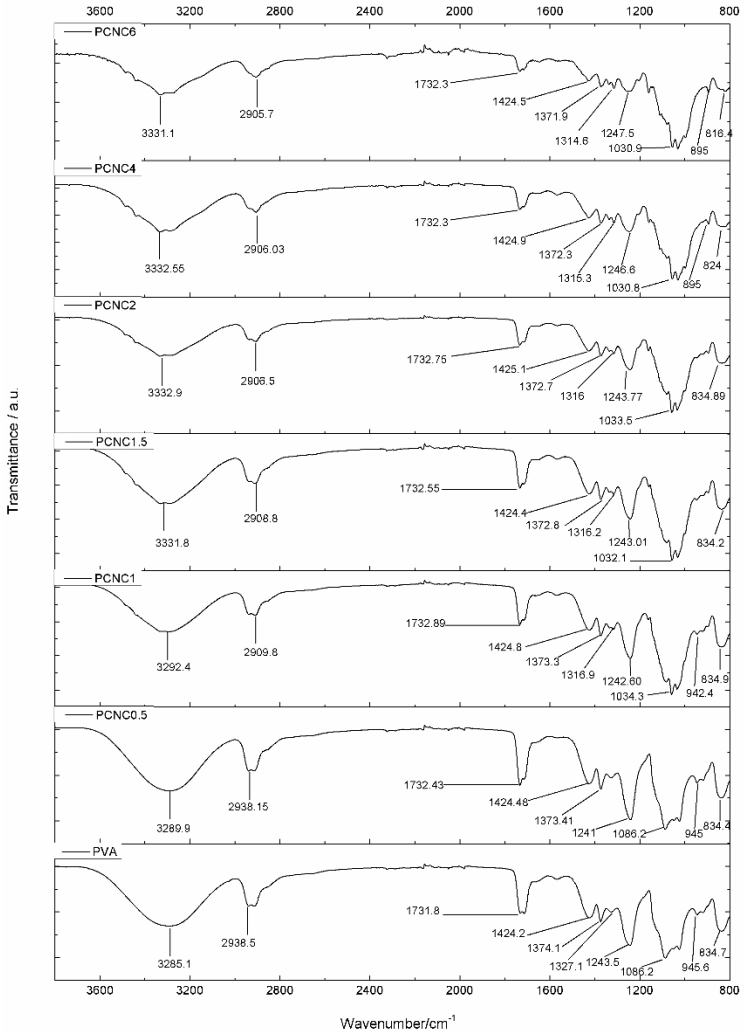

Fig. 2. Moisture uptake of PVA and PVA/CNC composite membranes at a,b) 53% RH, and c,d) 93% RH.

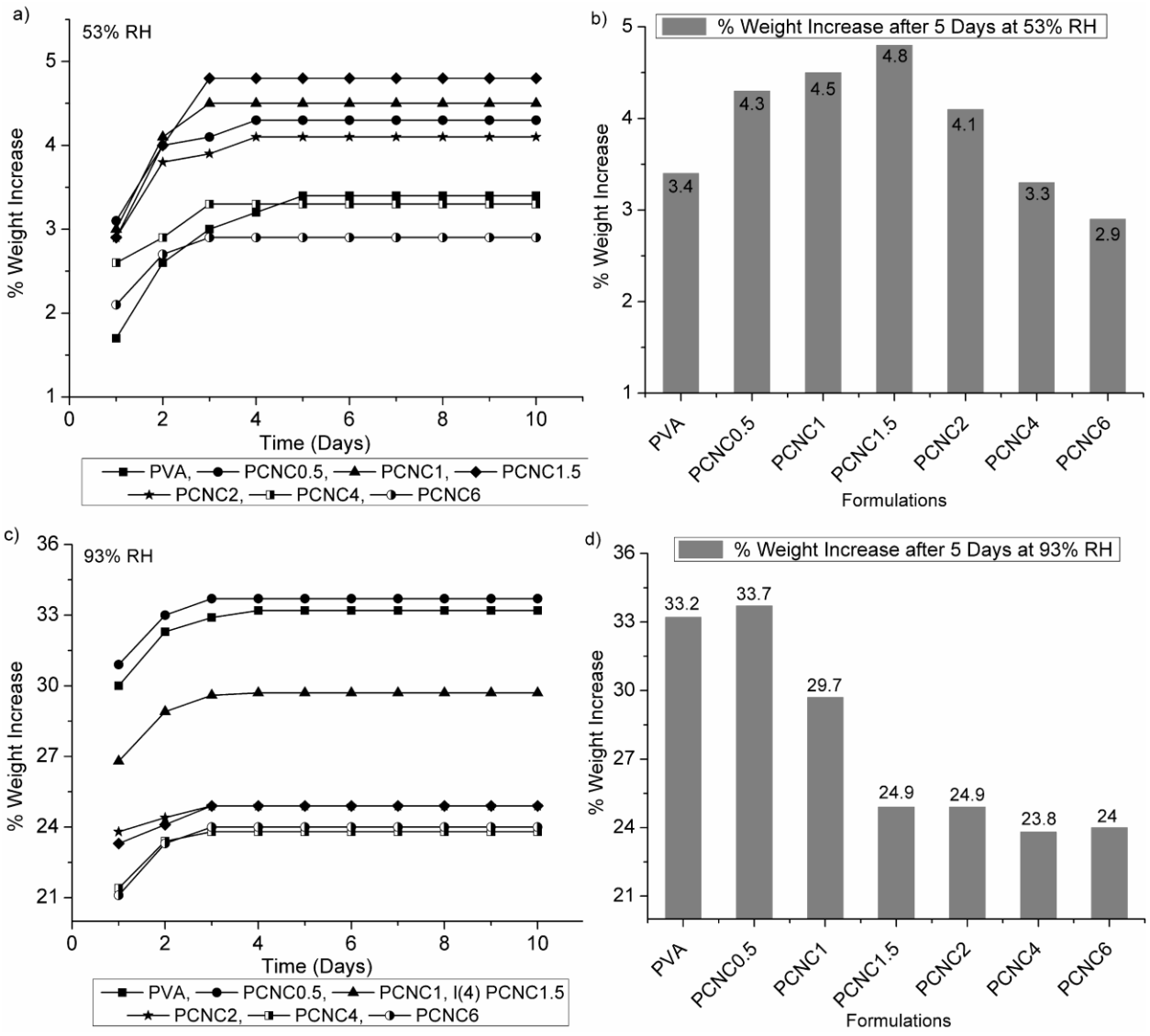

Fig. 3. X-ray diffraction patterns of PVA/nanocellulose composite membranes at 0%RH, 53% RH and 93% RH.

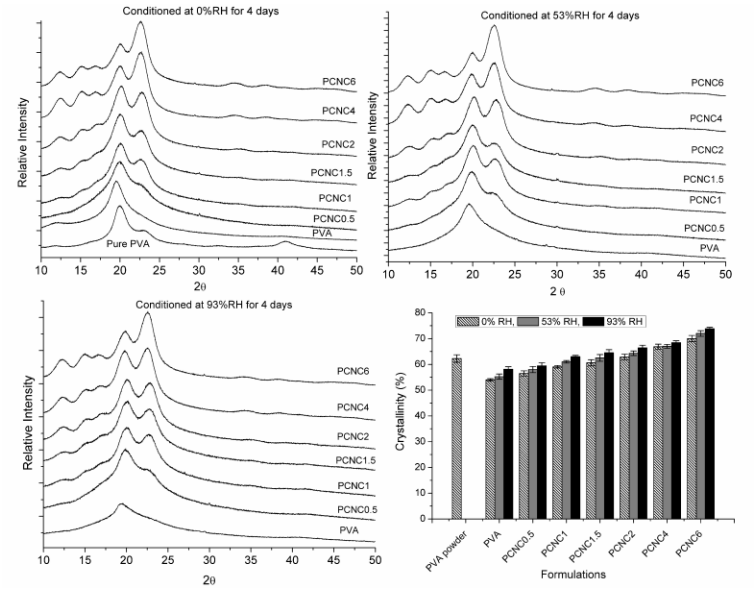

Fig. 4. SEM images of surface and cross-section of a) PVA membrane, b) PCNC1 and c) PCNC6

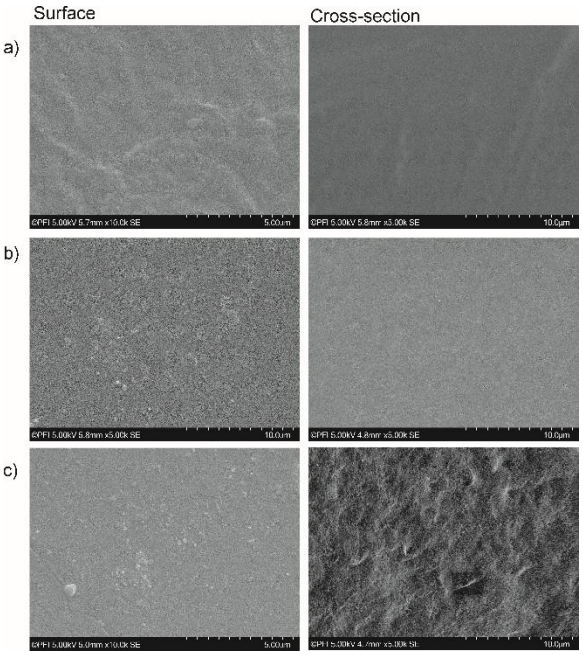

Fig. 5. TGA and DTGA curves of PVA/CNC composite membranes.

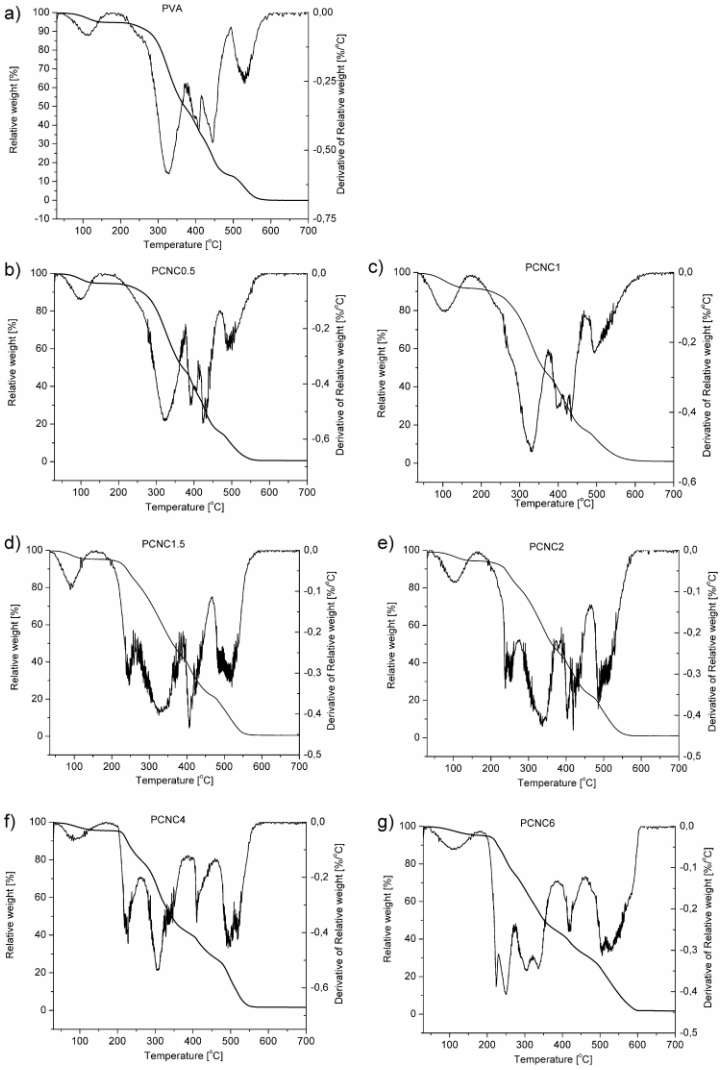

Fig. 6. DSC curves of PVA/CNC composite membranes.

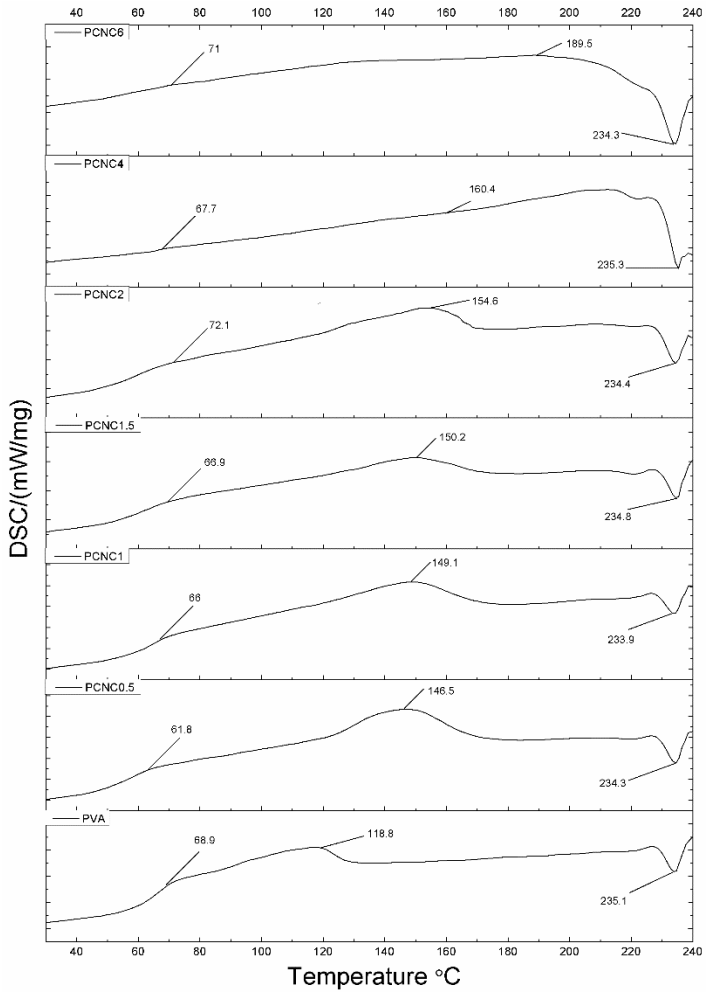

Fig. 7. Mechanical properties of PVA/CNC composite membranes at 0%RH, 53% RH and 93% RH a) Elastic modulus, b) Tensile strength, c) Elongation at break.

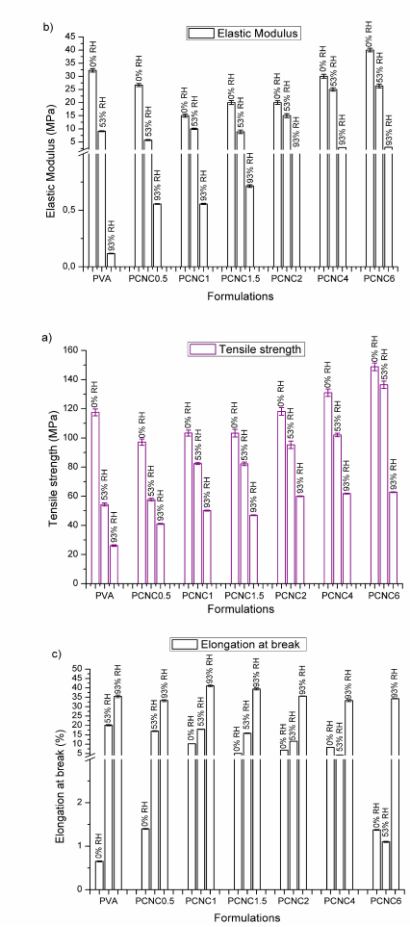

Fig. 8. Dynamic mechanical analysis curves of PVA/CNC composite membranes at a) Storage modulus and tan δ at 0% RH, and b) Storage modulus and tan δ at 93% RH

.

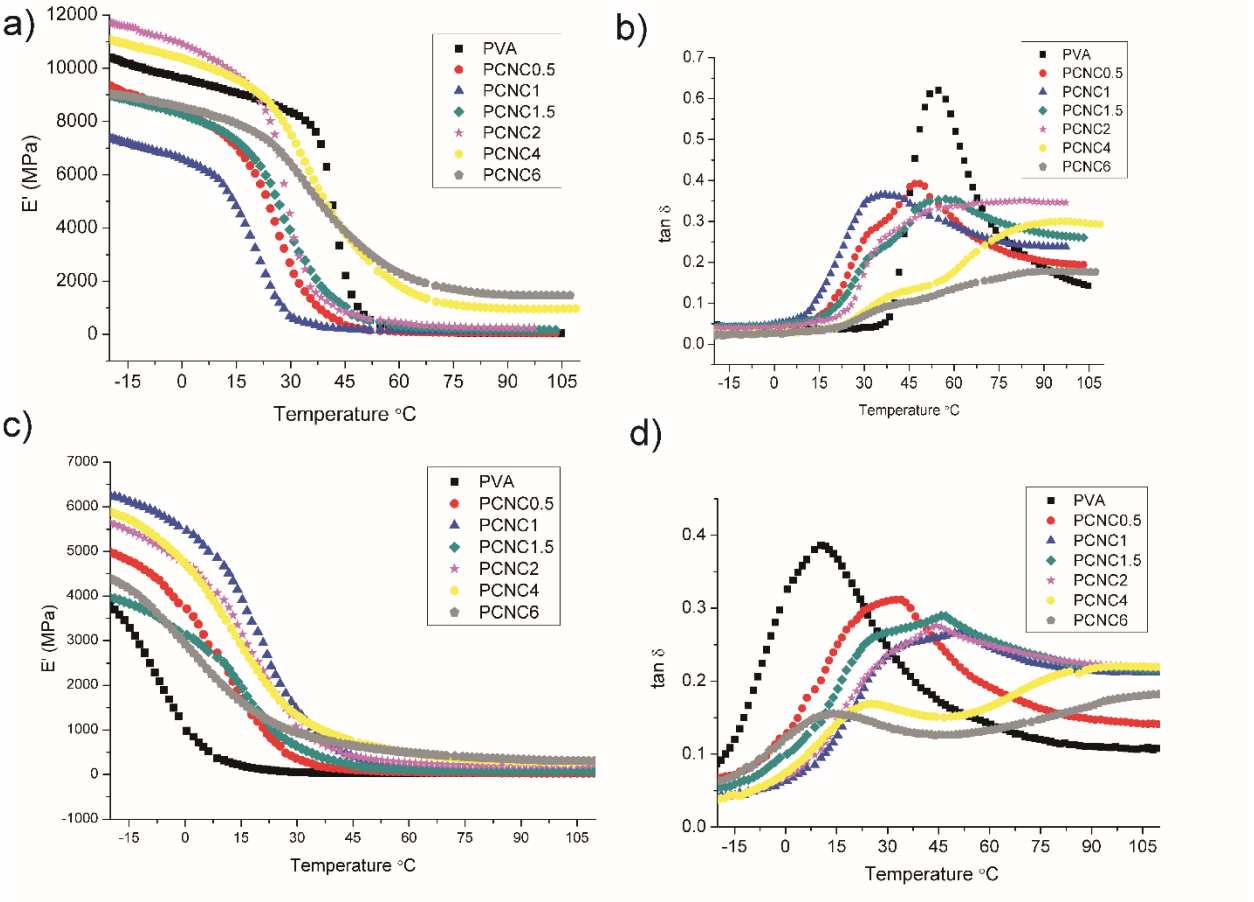

Table 1: Material codes and corresponding proportion of CNC in PVA matrix.

Film	**PVA mass (g)**	**CNC mass (g)**
PVA	2	-
PCNC-0.5	1.99	0.01
PCNC-1	1.98	0.02
PCNC-1.5	1.97	0.03
PCNC-2	1.96	0.04
PCNC-4	1.92	0.08
PCNC-6	1.88	0.12

Table 2. Dynamic mechanical analysis curves of PVA/CNC composite membranes

Sample	E' (Mpa) at 15 ± 5 °C and 0% RH	Tg (°C) 0% RH	E' (Mpa) at -8 ± 4 °C and 93% RH	Tg (°C) 93% RH
PVA	8371	54	3403	10
PCNC0.5	7873	47	4627	32
PCNC1	6234	35	5781	46
PCNC1.5	7462	55	3592	40
PCNC2	10600	55	5240	43
PCNC4	9782	42	5429	24
PCNC6	7873	41	3992	14